

# Exotic Rotational Correlations in Emergent Quantum Geometry

Craig Hogan

*University of Chicago and Fermilab Center for Particle Astrophysics*

Estimates are presented of exotic rotational correlations that arise if space emerges from Planck scale quantum elements with no fixed classical background. Directions in the classical inertial frame at separation  $R$  from any world line coherently fluctuate on a timescale  $R/c$  and angular scale  $(R/\ell_P)^{-1/2}$ , where  $\ell_P$  denotes the Planck length. The projection of the exotic correlations onto an interferometer signal correlation function is predicted exactly, for a light path of arbitrary shape: the signal variance is equal to twice the enclosed area divided by the perimeter or free spectral range, in Planck units. An experiment concept is sketched, based on reconfiguration of the Fermilab Holometer into an area-enclosing light path. It is conjectured that exotic rotational correlations, entangled with the Standard Model field vacuum, could account for the value of the cosmological constant.

## I. INTRODUCTION

It seems unavoidable that new exotic correlations in position, not predicted from standard theory based on continuous, infinitely divisible space and time, should occur if geometry is assembled from discrete elements at the Planck scale, or otherwise has Planck scale bounds on the number of degrees of freedom, as occurs in many theories of quantum gravity. Still, in the extensive literature on quantum extensions of general relativity[1–4], there is no generally accepted theory about the character of exotic quantum-geometrical position correlations in large systems.

Exotic correlations refer here to quantum correlations of geometry itself: that is, spatially coherent, nonlocally correlated phase displacements in quantum matter fields, and consequently on world lines of massive bodies. This kind of correlation is predicted to be negligible in standard field theory[5, 6], or in other theories of Planck scale effects[7–10], such as string theory, that assume relativistic quantum fields in a fixed classical background space-time on large scales. Exotic correlations can be imposed in the form of an assumed spectrum of fluctuations in the metric, with effects that resemble a background of gravitational waves[11–14]; although some of these may produce observable effects[15], they have not been shown to have this form in any quantum gravity theory.

Significant exotic correlations could however arise naturally in relational theories, in which all geometrical relationships emerge from a quantum system of Planck scale elements. In these theories, there is no *a priori* background space-time. The familiar components of geometry, a manifold of events in space and time described by a metric, appear as approximate features of a quantum system on scales much larger than Planck, but the exotic correlations are not in general the same as metric fluctuations. For example, Loop Quantum Gravity[1–3] predicts a quantized spectrum of geometrical area states that extends to large systems, a property that appears to imply new exotic positional correlations not described by a classical metric. However, there has been no generally accepted phenomenological model to connect these states with physical observables.

The aim of this paper is to create a precise, albeit partly heuristic, phenomenological model of concrete observables in this class of theories. Physical constraints in the emergent system strongly constrain the structure of correlations of matter fields and quantum geometry, and allow remarkably precise predictions of exotic signal correlations in some types of apparatus. This model will help to design and interpret experiments to seek concrete evidence that space-time is indeed a quantum system composed of Planck scale elements.

The model is based on the hypothesis that exotic correlations take the form of rotations, with directional uncertainty transverse to separation from any observer. It has been shown that a Planck quantum limit on directional information can lead to exotic “holographic noise” in the signals of interferometers, and may be measurable with suitably configured experiments[16–22]. Here, the exotic transverse correlations appear as specifically as rotational modes in the emergent space, associated with holographic departures from the classical inertial frame. The purely rotational symmetry, and holographically bounded information content, considerably restrict the range of possible phenomenology, and leads in some situations to unique predictions.

This form of correlation is motivated by the concept of emergent space-time, in which the projection of a geometrical quantum state hierarchically unfolds in a superposition determined by causal structure around the world line of an observer. In this model of the quantum state of the matter-plus-geometry system, an “observer” is the world line that defines the causal regions where the entangled quantum state projects onto matter and geometry subsystems, and hence onto an observable quantity. In the case of an interferometer, the 3D projection of the exotic geometrical correlation that enters into an observable signal is posited to be transverse to the vector from the location of the beamsplitter whose position and rest frame determine the signal. Previously, it was assumed[16–22] that the geometrical wave function was transverse in a plane defined by wavefronts of the fields used for the measurement, that is,

the plane normal to the propagation direction of light at the world lines where it has interactions with matter. The rotational hypothesis advanced here implies exotic correlations over an entire causal diamond, and ties the concept of emergence of inertial frames to a concrete geometrical picture of nonlocal entanglement of geometry and matter. This property is used explicitly in the signal correlation analysis below, which relates affine time around an interferometer circuit to causal diamonds defined by intervals of proper or clock time at the beamsplitter.

It is argued here that this form of exotic rotational correlations should arise if space emerges relationally from Planck scale elements, with no fixed background. In classical relativity, or any field theory embedded in a fixed classical background space, any change in directional orientation between two world lines is defined relative to an absolute, locally defined nonrotating frame. This inertial frame is exactly defined in principle, even on infinitesimally small scales. Of course actual physical systems are subject to quantum limits on what can be measured, but in standard theory, measurement of the inertial frame is limited by standard quantum mechanics[23], not by any limitation of geometry itself. If space itself is not a smooth classical manifold, but is a quantum system made of Planck scale elements, the situation on the Planck scale may be radically and qualitatively different from this standard theory. Classical directions on the smallest scales may not exist, since classical space emerges only as an approximation in large systems. As one approaches the position of a world-line, the non-rotating frame is less and less well defined relative to the classical frame. There is no such fundamental thing as an unchanging direction, and all observable quantities at the Planck scale, including direction, fluctuate wildly at the Planck frequency. In this case, small amplitude exotic rotational correlations, associated with coherent fluctuations in direction about a given world line, relative to the classical inertial frame, should also occur for separations and durations much larger than the Planck scale. Estimates of their statistical properties based on Planck scale holographic information content (for example, Eq. 22 below) suggest that exotic rotational correlations in large systems are indeed very small, but much larger than in standard theory. One can heuristically picture the correlations as arising from rotational quantum-geometrical or holographic noise in the inertial frame: spatially coherent fluctuations in direction that get smaller, slower and gentler on larger scales.

Some precise quantitative observable consequences of such exotic rotational correlations are calculated here. They should project into signals of interferometers, but only those in which which light travels in a path that encloses a large area, such as a Sagnac circuit[24, 25]. The most useful result is an exact correlation function for the signal in an interferometer of any shape (Eq. 35). The variance in the signal is equal to twice the area enclosed by the light path, divided by the perimeter, in Planck units. The exact choice of units depends on the theory of quantum gravity; one precise normalization is provided by the area quantization spectrum of Loop Quantum Gravity.

Exotic rotational correlations with the predicted spectrum could be measured by a superluminally sampled interferometer system with similar sensitivity to that already demonstrated by the Fermilab Holometer[26], but reconfigured to include transverse segments that enclose an area. A specific experimental concept is sketched as an example: for a square configuration 20 meters on a side, the computed spectrum predicts an interferometric phase shift jitter with an rms amplitude of 11 attometers, in a broad band of frequencies around 4 MegaHertz.

An even more speculative conjecture offered here is that exotic rotational fluctuations, entangled with the field vacuum, could shape emergent geometry on cosmic scales. In particular, it is proposed that the value of Einstein's cosmological constant  $\Lambda$  is fixed by the scale where the exotic rotational correlations entangle significantly with the strongly self-interacting Standard Model field vacuum. The spatial amplitude of exotic Planck correlation matches the strong interaction correlation length at a radial separation where rotational fluctuations produce an rms angular rotation rate— and heuristically, a universal rate of mean centrifugal acceleration— about equal to the observed rate of cosmic acceleration. It is shown below that within current experimental errors, the density of positional information is the same for cosmic expansion and the strong interaction vacuum— a close agreement in stark contrast to the wildly divergent estimate from quantum field theory with a Planck scale cutoff[27]. In this scenario, the value of the cosmological constant depends only on known scales of quantum gravity and the Standard Model.

## II. ESTIMATES OF EXOTIC QUANTUM GEOMETRICAL CORRELATIONS

### Planck Scale Correlations in Large Systems

The content of a quantum theory can be expressed as correlations between observable quantities[28, 29]. In standard physics, matter is a quantum system, while geometrical relationships are classical. However, it is generally thought that a quantum system also underlies space and time[1–4]. If so, the background quantum geometry should also produce quantum correlations among observable quantities, beyond those of quantum matter.

Quantum correlations have an inverse relation to the information in a system: they vanish in the limit of a continuous classical system, which has an infinite amount of information. Theoretical extrapolations from standard theory suggest that quantum gravity limits the amount of information available to a system of matter and geometry,

and therefore, creates new forms of correlation not predicted in standard theory. However, it is not known what form those correlations take.

Here we consider the hypothesis that quantum-geometrical correlations can be expressed as exotic correlations in the spatial positions of world lines, as traced by trajectories of massive bodies. These correlations can be distinguished from standard quantum correlations by precise measurements of positions of bodies in space. They carry significant, specific and quantitative information about the structure of new physics at the Planck scale.

We have previously considered one class of such measurements, those possible with Michelson interferometers[15–21]. Here, we consider a related but different class of possible correlations, associated with rotational modes, or pure changes of direction in space. In particular, we argue that measurements sensitive to the phase of radiation whose path encloses a large area may detect correlations due to the imperfect emergence, in a laboratory-scale system, of a local inertial frame from quantum relationships of Planck scale elements.

In an interferometer, a quantum-geometrical correlation is ultimately measured as the time domain correlation (or equivalently, its frequency-domain transform) of an observable  $x(t)$ , with dimension of length:

$$\Xi(\tau) \equiv \langle x(t)x(t+\tau) \rangle_t. \quad (1)$$

The quantity  $x$  is measured from a light intensity that depends on the phase difference between beams that travel through an arrangement of mirrors in space. It characterizes the departure from a perfectly classical, continuous geometry. A variety of estimates reviewed below suggest that quantum geometry in a system of size  $c\tau$  produces exotic correlations in position with magnitude roughly

$$\Xi(\tau)/c\tau \approx \ell_P, \quad (2)$$

where  $\ell_P = \sqrt{\hbar G/c^3} = 1.616 \times 10^{-35}$  m denotes the Planck length. They represent a measure of the (inverse of the) information density in the geometry. We refer to correlations of this magnitude as “exotic” Planck correlations because they are not produced in standard classical geometry. Experiments with interferometers— in particular, the Fermilab Holometer[26]— have shown that it is possible to measure position correlations with instrumental metrology at better than the Planck sensitivity in Eq. (2).

Such experiments can in principle probe Planck scale quantum degrees of freedom [15–22]. A signal is produced by light interference from a system of mirrors in a specific spatial arrangement. The time correlation of the signal, as in Eq. (1), depends on the detailed spatial layout of the apparatus, and the detailed character of the exotic 3+1 D position correlations. An experimental program with a variety of configurations can map out the structure of Planck scale quantum correlations and their relationship with properties of matter fields.

The projection operators for a given apparatus are not calculable in standard theory, since they depend on a phenomenology for a still-unknown theory of quantum geometry. On the other hand it is often still possible to predict the possible forms of correlation from the arrangement of mirrors in space, and to make quantitative tests of specific hypotheses about the geometrical correlations. These hypotheses necessarily lay beyond the framework of standard theory, but provide theoretical estimates of the density and character of information in a space-time system that can be compared with the magnitude and character of the correlations in data. In the following sections of this paper, we predict new, specific manifestations of exotic correlation associated with rotation and emergent direction. First however, we review estimates of the magnitude of exotic correlations from extrapolations of well tested physics.

### Gravitational Bounds on Matter Quantum Degrees of Freedom

A classical geometry is a continuous system, with an infinite density of position information. Significant deviations from this approximation are predicted at the Planck scale. A variety of theoretical estimates suggest that exotic correlations, originating from Planck scale quantum geometry, may have a magnitude in large systems that corresponds to position displacements much larger than the Planck length. Those estimates are reviewed here: first, general bounds on the density of information, and then, more specific indications that these should manifest in observable exotic position and direction correlations.

#### *Idealized Chandrasekhar Radius and Mass for Gravitating Systems of Relativistic Quanta*

It is useful to start by reviewing Chandrasekhar’s instability[30] in gravitating systems of relativistic quantum matter. Although these systems can be described without quantizing gravity itself, or even invoking the full apparatus of general relativity or concepts such as black holes, it is no accident that Chandrasekhar’s scales of mass and radius appear in other, more exotic contexts summarized below: they all invoke similar criteria that relate quantum states of

matter to global properties of a gravitating system. For both astrophysical systems and quantum field systems with gravity, the behavior changes qualitatively at this radius.

Chandrasekhar derived solutions for a spherical system of matter in hydrostatic equilibrium, so that gravitational force is in balance with a gradient in degeneracy pressure. He showed that the system becomes unstable when the mean velocity of the supporting particles, which in the case of a degenerate dwarf stellar remnant are mostly electrons, approaches the speed of light. Formally in his calculation, the radius of the equilibrium solution goes to zero. It is not necessary to invoke the concept of black holes; indeed, it is adequate to use a Newtonian approximation for gravity.

Suppose the mass is dominated by baryons whose mean number density  $n$  equals that of electrons. Denote their masses by  $m_b$  and  $m_e$  respectively. Let  $M$  and  $R$  denote the mass and radius of the system, so that

$$M \approx nm_b R^3. \quad (3)$$

(Exact numerical prefactors depend on the details of the equilibrium density profile; they do not affect our discussion and are omitted here.) At the onset of the instability, when the velocity of degenerate electrons approaches the speed of light,

$$n \approx (m_e c / \hbar)^3, \quad (4)$$

where  $c$  denotes the speed of light and  $\hbar$  denotes Planck's constant. This is also the approximate density of information—the number density of degrees of freedom of any field up to mass  $m_e$ .

The criterion of hydrostatic equilibrium is approximately that the total kinetic energy of the electrons is the same as the gravitational binding energy, and at the onset of instability this yields

$$R_{Chandra}^3 n m_e c^2 \approx G M_{Chandra}^2 / R_{Chandra}. \quad (5)$$

From these we derive the Chandrasekhar radius and mass at the onset of instability:

$$R_{Chandra} / \ell_P \approx m_P^2 / m_e m_b, \quad (6)$$

and

$$M_{Chandra} / m_P \approx m_P^2 / m_b^2, \quad (7)$$

where  $m_P = \sqrt{\hbar c / G}$  denotes the Planck mass. The same critical scales emerge from other kinds of quasi-equilibrium states dominated not by degeneracy pressure, but by thermal pressure; the stability depends on when the velocity of the particles that dominate the pressure approach the speed of light.

In this sketch approximation, the (critical maximum) mass  $M_{Chandra}$  only depends on  $m_b$ , which makes it clear why the masses of neutron stars nearly match those of white dwarfs. Indeed,  $M_{Chandra}$  sets the scale for all stellar-mass systems. The radius  $R_{Chandra}$  also depends on the lighter particle mass  $m_e$ ; lighter particles yield a larger critical minimum radius when collapse occurs, so that white dwarves are much larger than black holes of the same mass when they become unstable.

For the purposes of this paper, it is useful to define an idealized Chandrasekhar radius and mass, in terms of a single particle mass  $m$ , that applies if the gravitational mass and pressure support comes from the same particles:

$$R_C / \ell_P \equiv (m / m_P)^{-2}, \quad (8)$$

and

$$M_C / m_P \equiv (m / m_P)^{-2}. \quad (9)$$

For  $m$  about the mass of the neutron, these approximately give the radius and mass of a neutron star. Since  $R_C = M_C$ , the system is also close to the radius  $R_S$  of a black hole, for which  $R_S = 2M$  in Planck units.

While the Chandrasekhar mass (Eq. 9) has broad significance for shaping astrophysical systems, the idealized Chandrasekhar radius (Eq. 8) takes on a universal significance in the relationship of field states with quantum geometry. At larger separations, the effect of gravity significantly alters field theory, as shown in Fig. (1). The effect can be interpreted as entanglement of fields with quantum geometry—a breakdown of the standard assumption of classical geometry on large scales.

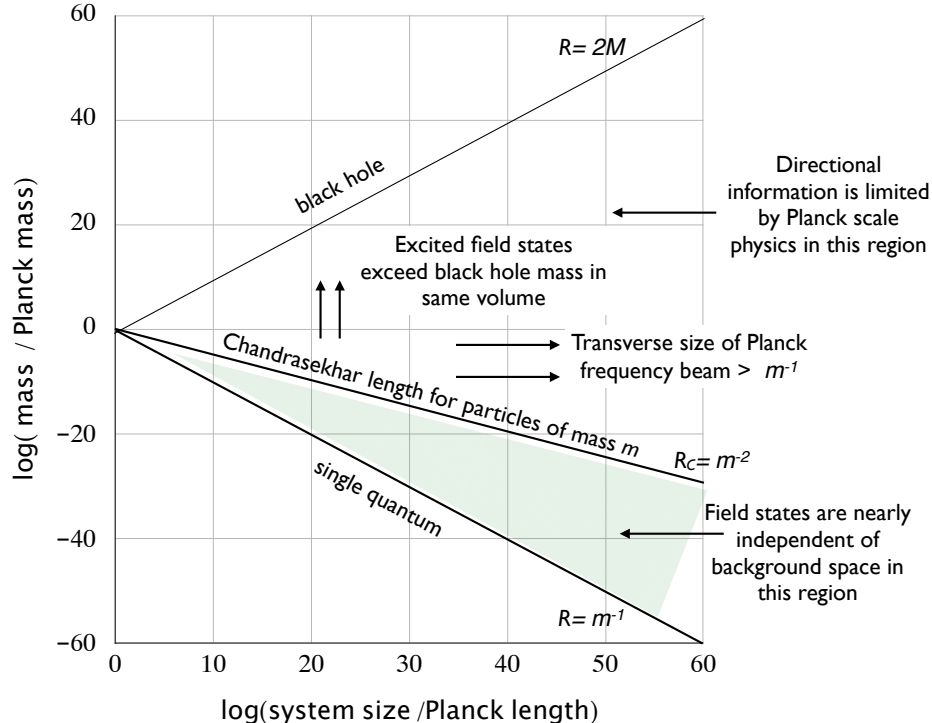


FIG. 1. Inconsistency of standard quantum field theory with gravity in large systems. The shaded region shows the sizes of systems where gravity requires only small corrections to field modes up to momentum  $mc$ ; above  $R_C(m)$  (Eq. 8), quantum geometry reduces the number of degrees of freedom for modes of mass  $m$  by a large factor. The mechanism proposed is the entanglement of fields with exotic geometrical states, which have correlations in transverse position of amplitude  $\Xi(R_C) \approx (\hbar/mc)^2$  at separation  $R_C(m)$ .

#### *Gravitational Constraint on Virtual States of a Field Vacuum*

To illustrate the effect, consider a model of matter based on a relativistic quantum field, such as those of the Standard Model, combined with gravity. An important difference from the system studied by Chandrasekhar is that the quantum system includes all possible states of the field, including nonzero occupation numbers for all of its modes.

Consider states of a field below some UV cutoff scale with wavelength  $\lambda = \hbar/mc$ . In a volume  $R^3$ , the field has about  $N \approx (R/\lambda)^3$  independent modes. In a state where each mode has mean occupation number of order unity, the number of particles per volume is about  $n \approx (mc/\hbar)^3$ , as in the Chandrasekhar system. Thus, in a volume with a size larger than Eq. (8), the excited field state has a mass larger than that of a black hole of the same size, which is of course an impossible physical state, inconsistent with general relativity.

This paradox suggests that even in a vacuum, exotic Planck scale quantum correlations somehow produce an “infrared cutoff” to field states of mass  $m$  at the idealized Chandrasekhar radius (Eq. 8), which of course is much larger than the Planck scale. Such an infrared constraint would not have been noticed in particle experiments[22, 31]. The effective cutoff from this entanglement is again the system size shown in Fig. (1).

#### *Holographic and Statistical Gravity*

Black holes were discovered as classical solutions in a classical geometrical theory, general relativity. However, an extensive literature on the theory of black holes suggests that general relativity has another formulation as an emergent statistical system, with a holographic information content determined by the Planck scale.

Classical black holes obey analogs of thermodynamic relations, where the entropy of a black hole is one quarter of the area of its event horizon in Planck units, and black holes radiate nearly as black bodies[32–36]. Thus, black holes

appear to be statistical systems composed of Planck elements, with a holographic information content proportional to area. Many thought experiments and precise examples of holographic mappings in various spaces suggest that this holographic property generalizes to any system with gravity, not just black holes[37–41].

Indeed, the equations of general relativity themselves can be derived [42–44] by requiring curvature to create geodesics that obey thermodynamic relations  $\delta Q = TdS$ , using geometry-related definitions of those quantities, such as holographic entropy density on horizons. In the thermodynamic-gravity view, entanglement of matter with geometry is thus naturally associated with gravitational lensing of geodesics, which in turn suggests entanglement associated with exotic directional correlations, as discussed below. At the Chandrasekhar radius given by Eq. (8), the directional information in matter and geometry, as related by Fermat’s principle, is the same: a wave front with this radius of curvature curves through one Planck length in a patch of size  $1/m$ .

The holographic entanglement of geometry with field states in asymptotically flat space should manifest differently from that in anti-de Sitter (AdS) space, a system often used to analyze holographic states. AdS space reflects both null and timelike trajectories back to any point of origin, in a finite characteristic time determined by the curvature radius of the space. In that system, significant entanglement of fields and geometry at large particle energies, for which the Chandrasekhar radius  $R_C(m)$  is larger than the AdS radius, appears in the boundary theory— the holographic dual of the bulk theory, rather than at large  $R$  as it does in flat space.

### Exotic Correlations of Transverse Position at Large Separations

The arguments just given provide estimates of the amount of information, and the scale of entanglement of geometry and field states. However, they do not directly reveal the origin or nature of the entanglement. Based on these estimates alone it is possible to imagine that the entanglement may be of a very subtle nature, and possibly not reveal itself in measurements of mirror positions. The following arguments suggest more specifically that new Planckian quantum behavior in large systems may appear as long-range, nonlocal geometrical correlations of the world lines of massive bodies. They take different complementary approximations to the emergent space but all approximately agree on the magnitude and character of exotic Planck correlation, related to a transverse width for the geometrical position wave function of a geometrical position operator  $\hat{x}$  that depends on separation  $R$  approximately as

$$\Xi(c\tau = R) \approx \langle \hat{x}_\perp^2 \rangle_R = R\ell_P, \quad (10)$$

or equivalently, a wave function of emergent direction with a separation-dependent angular width,

$$\langle \Delta\theta_P^2 \rangle_R \approx \langle \hat{x}_\perp^2 \rangle_R / R^2 = \ell_P / R \quad (11)$$

A consistent toy model of a quantum algebra to describe geometrical states with these properties is reviewed in Appendix (A).

### *Quantum Geometrical Information*

Quantum mechanics imposes a number of fundamental limits on the precision of position measurements[23]. One of these[45] enforces a minimum amount of energy associated with measurement of any time interval between events: the time it takes a quantum system to go from one state to an orthogonal state is greater than or equal to  $\pi\hbar/2E$ , where  $E$  is the expectation value of the energy of the system above the ground state energy. This result has been used to show[46] that in any volume there is a maximum number of distinguishable events, such that the density of clocks and signals used to measure their separation, GPS-style, not exceed the density of a black hole. In a spacetime volume of radius  $R$  and duration  $\tau$  in Planck units, the bound on the number of events is about  $R\tau$ . Since  $c\tau \approx R$  for a covariantly defined volume (such as a causal diamond), this is the same amount of information as the holographic estimates from statistical gravity just discussed. Indeed, this argument has been used as a statistical basis for general relativity[46]. Note that the area here combines spatial and temporal dimensions,  $R$  and  $\tau$ .

It is possible in principle that these measurement bounds might not apply to unmeasured degrees of freedom, if position information is subject to subtle squeezing. However, it does use an exact formulation of quantum information that applies specifically to event positions. It suggests that large scale exotic Planckian correlations indeed appear in measurements of relative positions of events and world lines, that could be measured by light reflecting off of macroscopic objects.

*Planck Diffraction Limit on Directional Resolution*

An estimate of directional spread from standard diffraction follows directly from the relativistic wave equation,  $\partial_\mu \partial^\mu \psi = 0$ . For waves of frequency  $\omega$  propagating in a beam—a stationary, monochromatic wave state proportional to  $e^{-i\omega t} \psi(x, y, z)$ , transversely localized in  $x$  and  $y$  and extended in  $z$ —the wave equation becomes

$$[\partial_x^2 + \partial_y^2 - 2i\omega \partial_z] \psi = 0, \quad (12)$$

the same equation used to model laser beams. The minimum transverse angular spread or diffraction limit for a Planck frequency beam[18, 19, 22], with  $\omega \approx m_P c^2 / \hbar$ , is thus:

$$\langle \Delta \theta_P^2 \rangle \approx \ell_P / R. \quad (13)$$

*In an emergent space-time, this angular resolution bound should apply not just to physical waves, but also to bandwidth-limited wave functions of position of world lines.* In this case the role played by sharp longitudinal boundary conditions (mirrors) in a laser cavity is played in emergent geometry by causal structure: the requirement that radial position and causal structure have Planck length precision at all separations. The degrees of freedom can be divided into radial information, which describes causal structure, and directional information, which describes two-dimensional angular orientation and transverse position. One factor  $R/\ell_P$  of holographic information content describes causal, longitudinal degrees of freedom; the other factor of  $R/\ell_P$  describes directional degrees of freedom. By contrast, in a full resolution 3D space the two directional dimensions on their own would comprise  $(R/\ell_P)^2$  degrees of freedom.

Directions in space may emerge from the Planck scale in such a way that exotic directional correlations of the emergent space on a scale given by Eq. (13). Field states cannot exceed the angular resolution of geometry, so they become strongly entangled with geometry at a separation where Planck diffraction matches the resolution of matter fields,  $\approx (m/R)^2$ ; that separation is given by the idealized Chandrasekhar radius, Eq. (8).

*Minimal Spreading of Wave Packets of Massive Bodies Over Time*

The directional blurring scale can also be derived from standard wave equations applied to quantum states of wave packets with Planck bandwidth[18–22]. In this estimation, wave functions of world lines of bodies of any mass spread at the same rate as those of particles of Planck mass. The scale can in this case be estimated starting from the standard wave function  $\psi(x_i, t)$  of a massive body in classical position and time. In its classical rest frame, a massive body obeys a 3+1-dimensional version of the paraxial wave equation (Eq. 12), with propagation in time in place of radial distance, and rest mass in place of frequency:

$$[\partial_x^2 + \partial_y^2 + \partial_z^2 - 2i(m/\hbar)\partial_t] \psi = 0. \quad (14)$$

Again like a laser beam, spreading of this wave function with time is unavoidable; any solution of duration  $\tau$  has a mean variance of position at least as large as

$$\langle (r(t+\tau) - r(t))^2 \rangle = \sigma_0^2(\tau) > \hbar\tau/2m. \quad (15)$$

the standard Heisenberg position uncertainty[47–50] for a body measured at times separated by  $\tau$ . In this wave picture, Heisenberg uncertainty is an exact analog of diffractive spreading in a light beam. Here, the sharp preparatory boundary condition—the equivalent of the mirror in a laser—is the preparation and measurement of the position state on spacelike surfaces at sharply defined times.

If emergent world line states correlate over duration  $\tau$  by about the same amount as the world line of a Planck mass body, the exotic correlation amplitude is about

$$\Xi(\tau) \approx \langle (x(t+\tau) - x(t))^2 \rangle \approx \ell_P c \tau / 2. \quad (16)$$

Suppose that this exotic world-line correlation has a pure transverse character. In the radial direction, the amplitude is limited by the standard quantum uncertainty for mass  $m$ , Eq. (15), but the transverse or directional uncertainty corresponds to that of a Planck mass body, so it is much larger than standard quantum uncertainty for  $m \gg m_P$ . Moreover, the transverse geometrical component is entangled for states of nearby world lines, so that quantum-geometrical part of the wave function is not independent from body to body; its spread leads to coherent fluctuations in direction.

One formalism to describe relational states of position in an emergent space-time composed of Planck scale elements is provided by Loop Quantum Gravity. It provides a concrete motivation, and normalization, for exotic geometrical correlations in large systems. Specifically, it predicts a discrete spectrum of quantum states of area that extends to large systems, with a holographic information content.

The discrete spectrum of area states is [1–3, 51, 52]:

$$A_j = 8\pi\gamma\hbar Gc^{-3} \sum_i \sqrt{j_i(j_i + 1)}, \quad (17)$$

where  $j_i$  are half-integers  $i/2$  for integers  $i$ . The Immirizi parameter  $\gamma$  has been computed to match black hole entropy for  $\gamma = \ln 2/\pi\sqrt{3}$  (see ref. [1], eq. 6.78). We adopt this result, recognizing that this is a prediction from just one particular fundamental relational theory. Since an important goal of an experimental program is to distinguish between theories, the absolute normalization should be regarded as a significant observable.

For large areas ( $i \gg 1$ ) we can write the eigenvalues (of so-called “main sequence” states) as

$$A_n \approx A_Q n^2 \quad (18)$$

for integers  $n$ , where

$$A_Q \equiv 2\pi\gamma\hbar Gc^{-3} \equiv \ell_Q^2 \quad (19)$$

is a fundamental Planck area unit. As discussed below, the natural fundamental length to adopt according to this formulation is not the standard Planck length  $\ell_P$ , but  $\ell_Q = \ell_P \sqrt{2 \ln 2/\sqrt{3}} = 0.895\ell_P$ . The difference between adjacent area states is

$$A_{n+1} - A_n \approx 2A_Q n. \quad (20)$$

Notice that the spacing grows with  $n$ . Thus for larger areas, each area eigenstate is bigger than the last by much more than a single Planck area pixel. For a system of area  $A = R^2$ , the difference between adjacent states is

$$\Delta A = 2\sqrt{A_Q A} = 2R\ell_Q. \quad (21)$$

It is natural to identify this quantity with the exotic position correlation amplitude on each scale,  $\Xi(\tau = R/c) \approx \Delta A(R)$ . The areal quantization reflects the same blurring or loss of relative positional information on large scales that appears in wave equation solutions, holographic information constraints, and other “infrared” departures from field theory reviewed above. It explicitly captures an essential nonlocal feature of geometrical states: that the positional relationships of the geometry itself depend on separation, and degrade over large areas.

### III. EXOTIC ROTATIONAL CORRELATIONS AND FLUCTUATIONS

#### Quantum Fluctuations of Inertial Frames: Newton’s Bucket at the Planck Scale

The concept of absolute space was invented by Isaac Newton. In a “Scholium to the Definitions” in the *Principia* [53–55], Newton describes a thought experiment with a rotating vessel of water. The curved surface of the water demonstrates the physical reality of absolute space: “This ascent of the water shows [indicat] its endeavor to recede from the axis of its motion; and the true and absolute circular motion of the water, which is here directly contrary to the relative, becomes known [innotescit], and may be measured [mensuratur] by this endeavor.” Newton thereby differentiates rotation from other types of relative motion: “And therefore this endeavor does not depend upon any translation of the water in respect of the ambient bodies, nor can true circular motion be defined [defineri] by such translation. There is only one real circular motion of any one revolving body, corresponding to only one power of endeavoring to recede from its axis of motion, as its proper and adequate effect; but relative motions, in one and the same body, are innumerable, according to the various relations it bears to external bodies, and like other relations, are altogether destitute of any real effect, any otherwise than they may perhaps partake of that one only true motion.”

Newton realized that are two different ways of telling whether a direction to a body is changing. One way is local: a change of direction causes centrifugal acceleration in the (rotating) frame in which the direction is not changing, as in the rotating vessel of water. The other way is to compare with very distant bodies. The agreement between these



two is fundamental and profound. Ernst Mach pointed out that physics needs to explain it, which inspired Einstein in the development of relativity theory.

Today the coincidence seems less profound, or at least less puzzling, because general relativity explains it with a complete, rigorous and well tested account of the classical physics of space, including a precise notion of absolute space. We now know that distant matter (Newton's "ambient bodies") actually does directly affect local space: its gravitational field influences the local nonrotating frame, via gravitomagnetic frame dragging. (In cosmological solutions, distant matter even nonlocally defines a preferred cosmic rest frame of motion at any given event, although that cannot be measured locally.) Thus in classical physics, no additional theory is needed.

However, it is a challenge for a quantum theory of gravity to account for the coincidence of local and global frames. In a fully quantum space-time[1–3], all positions and motions, indeed all observables, have to be relationally defined within the quantum system. There is no absolute reference standard to define the frame; there are only elements of the quantum system, starting with the Planck scale. In the quantum context, it is necessary to reconcile the coincidence with quantum indeterminacy and nonlocality.

Relativity preserves Newton's fundamental distinction between translations and rotations. Lorentz invariance dispenses with absolute motion through space as a local observable, but retains an absolute local definition of rotation: at every event on a world line, there is an absolute, nonrotating inertial frame. The rate of change of any direction is defined relative to a property of local space. This relationship is still classical, even for quantum systems: there is no relational quantum theory to explain how the orbital states of atoms "know about" matter in distant galaxies, to determine what states have zero angular momentum. In standard quantum theory, that relationship is still established via absolute, classical space.

Imagine shrinking Newton's rotating vessel to a Planck size. In modern standard theory, *as far as space is concerned*, the Planck size vessel works much the same as Newton's. The classical local inertial frame, which defines rotation, provides a complete (albeit classical) account of its relation to distant matter. This nonrotating frame is precisely defined by the classical geometry, and hence also in quantum field theory, even at the Planck scale.

Newton could well have imagined his bucket shrinking to infinitesimal size, with no modifications to his concept of absolute space. However, in modern standard theory, the bucket itself (as opposed to the space it inhabits) is governed by quantum mechanics. A bucket of any type of matter of Planck size has about the same mass, size and spin as a black hole, and as a single elementary particle. Its angular momentum is a superposition of quantum states, as described by the angular momentum algebra. It can have a definite spin about at most one axis; the other components are indeterminate. Thus, the Newton bucket experiment cannot be performed with arbitrary precision; the rotation rate is indeterminate by about a radian per Planck time.

Thus standard theory is in the awkward position of positing a classical inertial frame, a property of absolute space that cannot possibly be defined or measured, even in principle, below the Planck length. Ineed, standard relativistic frame dragging insures that this indeterminacy applies not just to the matter, but also to the geometry, so there cannot be a classical local inertial frame. The indeterminacy becomes less acute in larger systems, but even then the performance of a bucket experiment is subject to fundamental quantum uncertainties in the matter used for the experiment. It only make sense to posit classical behavior of space to the extent that it can be measured[23, 56].

The solution is to posit a system based on a quantum positional relationship between world lines. This feature is built into relational, emergent theories, in which world lines, and inertial frames, emerge gradually in systems much larger than the Planck length. In a Planck scale volume, a relational or emergent theory provides no absolute frame for a vessel to refer to; its local rotation rate is defined only with respect to nearby elements, all of which individually have Planck scale indeterminacy in their wave functions. The inertial nonrotating frame on the Planck scale is again indeterminate, leading to fluctuations in the rate of change of direction of the order of the Planck frequency. For large separations, a long interval on a world line allows a rotational relationship between world lines to be defined by averaging over a larger region.

For large systems and long times, the Planck scale uncertainty and fluctuations average out, but the averaging is not perfect. Even large systems must display small residual correlated fluctuations in direction: the system displays small, exotic rotational correlations. It is proposed here that the overall quantum system of matter and geometry approaches the well known classical limit of approximately absolute space in a way that is uniquely constrained by the symmetries of space, and by the requirement of saturating the holographic bound on information in causal diamonds over long time intervals. The scaling of the uncertainty has been estimated above: the directional resolution of the overall system on all scales is given by the Planck diffraction bound. In the following, we evaluate some of the phenomenological consequences.

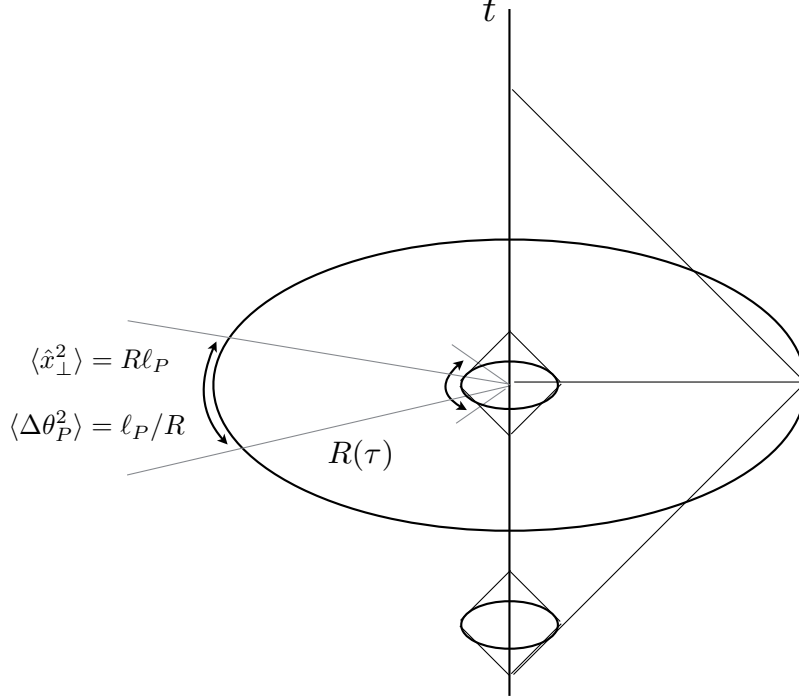


FIG. 2. Rotational fluctuations in a large volume of space emerging from Planck scale elements. Transverse position and directional width of the geometrical wave function are shown on a 3-surface in the rest frame of a particular world line, at a particular proper time  $t = 0$ . The light cone of a Planck scale 4-volume (center) shows a large uncertainty in direction because there is no fixed reference frame on that scale. As space emerges over larger intervals of proper time, information about the nonrotating frame is correlated with distant parts of the system by hierarchical entanglement (see also Fig. ??). Along a particular world line, the directions collapse in nested light cones; correlations between times separated by interval  $2\tau/c$  extend to a separation  $R = c\tau$ . The space within the bounding 2-sphere of radius  $R$  undergoes coherent rotational fluctuations relative to the space outside. The rotational state of the entire system must collapse self consistently, requiring entanglement of states around all enclosed world lines. Directions within that surface rotate coherently, relative to more distant world lines, fluctuating with variance  $\langle \theta_P^2 \rangle = \ell_P/R$  on a time scale  $\tau = R/c$ . The correlation  $\Xi(\tau)$  in an interferometer signal is determined by the mapping  $R(\tau) = |x_i(\tau)|$  defined by the light path, combined with the geometrical projection of the transverse directional variance.

### Quantum States of Matter and Geometry with Exotic Rotational Correlations

Matter and geometry refer to different properties of one quantum system. To a very good approximation in experiments to date, they refer to nearly-separable subsystems. The goal here is to find a way to detect the exotic correlations associated with their entanglement.

Matter refers to field-like properties of the system, that is, spatially localized field amplitudes and derivatives, and geometry refers to position-like properties, that is, directions, radial, and temporal separations. As shown above, theory suggests that the quantum system underlying space contains a limited, holographic amount of information, and that this bound affects the behavior of field states in large systems. The hypothesis of this paper is that the holographic bound particularly affects directions in space. Radial separations, and the causal structure defined by null causal diamonds associated with intervals on any world line, retain very nearly their classical structure.

This idea fixes the form of the exotic entanglement of matter and geometry in large systems. Even with no dynamics or Lagrangian for the system, this hypothesis is sufficiently precise to calculate certain properties of the correlations and fluctuations. It leads to a specific scenario about how emergence works, and about the spatial character of the exotic correlations on large scales.

With this hypothesis, radial directions around any world line have a special significance. The null radial trajectories define causality in all directions, and define a particular set of eigenstates. This projection of the quantum system

is determined by a choice of world line or timelike observer. In the emergent space, spatial structure is defined by intersecting light cones from the ends of any interval on the world line, called causal diamonds. World lines, intervals of proper time, and causal diamonds represent invariant emergent geometrical objects. In the emergent system, there is no fixed background space to define an inertial frame. From one moment to the next, the situation depends only on previous relationships. The causal dependences of rotation around a world line are mapped out by the light cones emanating from each event. The total geometrical state of a system includes entanglement of all of the nested causal diamonds, and the total variance in position is the sum of variances from the nested diamonds (see Figs. 2, ??).

The effect can be thought of as a quantum differential rotation of space: everything closer than  $R$  rotates relative to everything more distant than  $R$ , by a very small amount. It is helpful to visualize the fluctuations as a sum of coherent discrete transverse spatial displacements, or quantum-gravitational twists of space, associated with discrete displacements in time. The amplitude corresponds to a Planck scale diffraction bound on directional resolution in space, or to a discrete Planck random walk in transverse position. On a null trajectory from a distant source to an observer, for each Planck step, space experiences a random transverse displacement from the classical trajectory, in which it shares common with other radial trajectories at the same  $R$ . The exotic correlation arises from the sum of coherent transverse displacement at the 2D boundaries of the nested causal diamonds.

In the quantum states of an interferometer, fields are entangled with geometry. The measured radiation depends on the phases of light incident on the beamsplitter, which combines geometrical information from macroscopically different paths through the space[47–49]. The projection of geometrical quantum states is determined by the true causal structure of the space, the therefore by the transverse components to the observer’s radial direction. The relationship between the two is analyzed in next section to compute the effect on an interferometer signal.

### *Behavior of Exotic Rotational Fluctuations in Large Systems*

Like zero point fluctuations of a field excitation in a vacuum, this quantum “motion” represents a quantum system with a nonzero width of a wave function that has a zero mean. In this picture, the zero point refers to a stationary direction in the classical nonrotating frame. A quantum relationship with matter out to the cosmic horizon prepares the global state and defines zero rotation. A zero net rotation state is defined by the classical geometry, but nearby there is a nonzero quantum variance that depends on distance from an observer. The wave function width is identified with the exotic correlations and fluctuations.

Directional degrees of freedom are subject to the usual holographic bounds on information, so the above estimates of directional variance lead to an estimate of the exotic directional correlations and their associated fluctuations, as shown in Figure (2). The exotic correlation and rotational displacement variance at separation  $R$  from an observer are about

$$d\Xi_R(\tau)/d\tau \approx (d\langle x_\perp^2 \rangle/dR)(dR/d\tau) \approx c\ell_P. \quad (22)$$

The rotational displacement is coherent in all directions from the observer at a constant radial separation defined by its causal structure— that is, on a 2+1-D tube of spacelike 2-surfaces swept out in time by causal diamonds with fixed sizes  $R = c\tau/2$ . For calculational simplicity, in this paper we focus on results in nearly-flat space relevant for experiments, but the formulation based on causal diamonds should generalize covariantly to curved spaces. A toy model of 3D holographic quantum positional states, summarized in Appendix (A), based on the 3D spin algebra, provides an example of a consistent holographic model of quantum position states in 3D. We use classical space-time for the time projection, as in Eq. (22). Since the states used are in 3D instead of 4D, time evolution is still treated heuristically, both here and in the calculation of interferometer response below.

We can describe the effect as statistical fluctuations in rotation of the inertial frame around each axis. An ordinary rotation about a body at the origin corresponds to transverse components motion  $dx_i/dt$  of a body at  $x_k$  according to the classical relation,

$$dx_i/dt = \epsilon_{ijk}x_k\omega_j, \quad (23)$$

where  $\omega_j$  is the rotation rate for component  $j$ . In the exotic fluctuations, each component of rotation of a 2-sphere of radius  $R$  has fluctuations with

$$\langle \omega_i^2(R) \rangle \approx c^2\ell_P R^{-3}. \quad (24)$$

All transverse displacements on a 2-sphere are self consistent according to the classical relation Eq. 23. That is, each component of rotational fluctuation determines an entangled motion across the whole sphere. In the same way that spins of quantum particles sent in opposite directions are entangled, in this case, the rotation of all the enclosed world

lines and causal diamonds are entangled. The projection of the states depend on the radial trajectories pointing back to the observer's world line.

The effect connects properties of states over an enormous range of timescales: the tiny displacement  $\approx R^{1/2}$  in Planck units, a coherence time  $\approx R$ , and an inverse angular rotation rate  $\approx R^{3/2}$ . The fluctuation coherence time in a laboratory setting— about a light crossing time— is less than a microsecond, even though the rotation rate is only about one radian in ten thousand years.

Exotic rotational correlations thus create the directional entanglement between geometry and field degrees of freedom indicated by the arguments of the previous section. The geometrical state is the same for all field modes; for modes of a each scale, entanglement becomes gravitationally significant beyond the corresponding idealized Chandrasekhar radius  $R_C$ . But even at smaller radii, states of all matter fields inherit small phase shifts from states of geometry.

#### IV. EXOTIC ROTATIONAL SIGNAL CORRELATIONS IN INTERFEROMETERS

For distances much larger than the Planck length, the effect of the fluctuations in single-particle interactions is small, and it is very small at laboratory particle energies, which are less than about  $10^{-16} m_P c^2$ . Interferometry by contrast uses very large numbers of particles to make a coherent, collective nonlocal position measurement of wave positions, with precision much smaller than a wavelength. The in-common transverse displacement on all fields at the laboratory scale is on the scale of attometers, an amplitude which may be detectable in precision interferometry.

##### Exotic Correlation in an Interferometer Signal

An interferometer maps the world lines of a set of mirrors in space and time onto a single time series,  $x(t)$ . The effect of quantum geometry on its correlation function  $\Xi(\tau)$  depends on the path taken by the light through space-time before the signal is produced, and in particular, on its interaction with world lines of massive mirrors that change its direction. Thus, the correlation is determined by the arrangement of the mirrors in the apparatus. The measured quantity in an interferometer is the time correlation function of the dark port signal,

$$\Xi(\tau) \equiv \langle x(t)x(t+\tau) \rangle_t \quad (25)$$

where  $x(t)$  represents the phase difference between beams arriving and interfering at the beamsplitter, measured in length units.

Consider an interferometer in the local inertial frame of the beamsplitter, the world line where the wave function of geometry interferes with that of measured radiation. In this frame, based on general considerations of holographic scaling and statistical isotropy, we posit the following form for the 3D exotic position correlation tensor at a single time:

$$\Xi_{ij}(x_k, \tau = 0) \equiv \langle x_i(x+x_k)x_j(x) \rangle_x = \epsilon_{ijk}x_k\ell_P, \quad (26)$$

where  $x_i, x_j$  represent exotic position displacements,  $x_k$  denotes a 3D separation vector, indices run from 1 to 3, and  $\epsilon_{ijk}$  represents the antisymmetric 3-tensor. This form corresponds to a consistent noncommutative quantum algebra of position operators with a holographic density of degrees of freedom — a rotational model of quantum geometrical states, as in Appendix (A). It vanishes in the classical (or fixed-background space) limit.

This hypothesis is sufficient to derive the 1D exotic correlation in an interferometer signal. Exotic correlations are related to exotic rotational fluctuations by the standard geometrical relation,  $\omega_j dx_i/dt = \epsilon_{ijk}x_k$ , and rotation is related to signal in the standard way for an interferometer. A functional of the apparatus light path  $x_i(\tau)$  determines a function of  $\tau$  that depends on  $\epsilon_{ijk}x_k\ell_P$  in the same way as the exotic 3D correlation tensor at each point on the path.

Consider a Sagnac interferometer, where the path of light is a closed circuit. The light follows the same path in two directions and the signal records their phase difference at the beamsplitter. Let  $\tau^+$  and  $\tau^-$  denote affine parameters along the path in the two directions. Denote the classical path of the interferometer in space, in the rest frame of the beamsplitter, by  $x_i^+(\tau)$  and  $x_i^-(\tau)$ , in the two directions around the circuit. Here  $i = 1, 2, 3$  again denotes the 3D spatial indices, although below we will assume a planar apparatus for simplicity. The functions  $x_i^+(\tau)$  and  $x_i^-(\tau)$  can be visualized as the trajectories of “tracer photons” in each direction around the circuit; they map positions on the circuit in 3-space to points on an interval on the real line,  $(-P_0, +P_0)$ , where  $P_0$  denotes the perimeter of the circuit, the origin maps to the beamsplitter, and  $\tau$  represents a time interval in the proper time of the beamsplitter. The effects of quantum geometry on the measured correlation  $\Xi(\tau)$  depends only on the classical path, defined by  $x_i^+(\tau)$

and  $x_i^-(\tau)$ , the positions of a pair of tracer photons that begin and end their circuit at the same time. The tangent vector to the path in each direction is  $\partial x_j^\pm/\partial\tau$ .

It will be convenient to express a general form for the functional dependence of  $\Xi(\tau)$  on the classical path in terms of the ‘‘swept-out area’’,  $A(\tau)$ , similar to the concept used in Kepler’s second law of planetary motion. Define  $A_i(\tau)$  as an oriented area in the inertial rest frame, swept out by lines between the beamsplitter and the tracers in the two directions (see Fig. 3). The areas from the beamsplitter to the two tracers change as:

$$dA_i^+/d\tau = \epsilon_{ijk}[x_k^+(\tau)dx_j^+/d\tau] \quad (27)$$

$$dA_i^-/d\tau = \epsilon_{ijk}[x_k^-(\tau)dx_j^-/d\tau]. \quad (28)$$

These quantities are completely determined by the geometrical configuration of the apparatus.

In general a transverse swept area can also be defined from the swept area between the two tracers, adding additional cross terms:

$$dA_i^\times/d\tau = \epsilon_{ijk}\frac{1}{2}[dx_j^+/d\tau + dx_j^-/d\tau][x_k^+(\tau) - x_k^-(\tau)]. \quad (29)$$

This component corresponds to shear, rather than rotation about the beamsplitter, and is assumed to vanish. The exotic correlation just depends on a combination of the two terms directly related to rotation about the observer/beamsplitter world line, Eqs. (27) and (28). This assumption is testable: if present, the shear terms would be detectable in a Michelson interferometer with straight arms[15, 21], which is not sensitive to the rotational terms. Experiments in both configurations would distinguish the modes, and explore the full character of transverse exotic position fluctuations.

#### *General Formulae for Exotic Rotational Correlations in a Planar Interferometer*

The exotic correlation amplitude in the signal is the projection of the exotic transverse position correlation onto the apparatus. The relations between  $dA_i^\pm(\tau)/d\tau$ ,  $x_k^\pm(\tau)$  and  $dx_j^\pm/d\tau$  provide a convenient way to project the exotic correlation  $\epsilon_{ijk}x_k\ell_P$  on each hypersurface to form an invariant function of  $\tau$  alone.

The projection can be visualized geometrically (Figs. 3, 4). Assume for simplicity a planar apparatus, and thereby suppress directional indices for  $A_i$ . The essential assumptions are just the holographic scaling of transverse position correlations, and the standard geometrical relations between  $R$  and  $\tau$ . The swept area rate  $dA/d\tau$  is proportional to separation from the origin at any point on the path, and to the projection of the path on the transverse direction at that point. Denote the angle between the light path tangent and position vectors by  $\theta'(\tau)$ . This angle determines the affine mapping and the swept area via

$$dA/d\tau = R(\tau) \sin \theta'/2, \quad (30)$$

where  $R(\tau) = |x_i(\tau)|$ . The exotic signal correlation at each  $\tau$ , apart from a constant offset fixed by the boundary condition determined by global layout of an interferometer, is the projection of the exotic 3D transverse position variance (Eqs. 26, A13) onto the light path:

$$(\Xi(\tau) + \text{constant}) = \langle \Delta x_\perp^2 \rangle_{R(\tau)} \sin \theta' = \ell_P R(\tau) \sin \theta'. \quad (31)$$

The swept area rate is then simply related to the signal correlation by

$$(\Xi(\tau) + \text{constant}) = 2\ell_P dA/cd\tau. \quad (32)$$

Equation (32) applies separately to each arm or leg of an interferometer of any shape. The full correlation function depends on the overall layout. For the specific case of a Sagnac interferometer, define the total swept area  $A_\pm(\tau)$  as a sum of the contributions from both directions, so that

$$|dA_\pm/d\tau| = |dA^+/d\tau + dA^-/d\tau|, \quad (33)$$

and the total physical enclosed area is

$$A_0 = \frac{1}{2} \int_{\tau=0}^{P_0} d\tau dA_\pm/d\tau \quad (34)$$

when integrated over the total perimeter  $P_0$ . Adding the contributions from the two directions in Eq. (32) then leads to the following formula for exotic correlation in a planar interferometer of any shape:

$$\Xi(\tau)/\ell_P = \Xi_0/\ell_P - |dA_{\pm}(\tau)/cd\tau|, \quad (35)$$

where the correlation at zero lag,

$$\Xi_0 \equiv \Xi(\tau = 0) = 2A_0\ell_P/P_0, \quad (36)$$

gives the total mean square phase variation from the exotic correlation in length units. This constant is determined by the requirement that the correlation integrates to zero for  $|c\tau| > P_0$ , so that the average rotation vanishes in the classical limit of zero frequency. A specific example of the predicted correlation function for a square configuration is shown in Fig. (5).

The general formula (Eq. 35) respects the symmetries expected for an emergent geometry. It has the correct spatial scaling and transformation properties to describe the 1D time domain correlation for a planar interferometer of any shape. It also makes physical sense; for example, in sections of the circuit where light is not interacting with matter, the path is straight, so that  $|dA_{\odot}(\tau)/cd\tau|$  is constant for corresponding intervals of  $\tau$ . Thus as expected, the correlation is constant over those intervals; the phase of radiation is not affected by trajectories of emergent world lines it does not interact with. At reflections where the rotational position of the mirror affects the phase of the light (that is, where the mirror surface normal is not in the radial direction), the signal correlation changes value discontinuously, as expected from exotic rotational correlations in the positions of the mirrors.

#### *Other Experiment Layouts and Cross-Correlation Between Interferometers*

The Sagnac layout illustrated is not unique: the same derivation applies for any layout with an enclosed area, such as a Michelson interferometer with a bent arm. The derivation above can be boiled down to a simple conjecture: the swept-area formulas, Eqs. (35) and (36), gives the full form of the function,  $\Xi(\tau)$ , for any interferometer. In the general case, to satisfy the integral constraint, the perimeter  $P_0$  corresponds to the total affine path length, that is,  $f_0 = c/P_0$ , where  $f_0$  denotes the free spectral range.

The nonlocal character of the exotic correlations provides opportunities for experiments to distinguish them from ordinary sources of environmental position noise. For example, two interferometers close to each other, with overlapping areas, should be almost entirely entangled, and show a cross correlation almost the same as their individual  $\Xi(\tau)$ . However, if one of them has a layout with zero area, say from folding the arms back to the beamsplitter, the exotic correlation disappears. The formalism here generalizes to computations of cross correlations between interferometers due to entanglement, given by the synchronous overlap between their swept areas.

#### *Normalization from Loop Quantum Gravity*

Physically, the behavior derived here corresponds to quantum correlation associated with quantization of an enclosed area emerging from Planck scale subunits. The correlation  $\Xi(\tau)$  depends on classical area and perimeter in Planck units. Exactly what are the appropriate units to use?

The area quantization from Loop Quantum Gravity described above (Eq. 19) has an exact normalization derived from the entropy of black hole states that can be used to set an absolute normalization for the correlation function. For definiteness, consider a square arrangement with sides  $L$ . For a square, Eq. (18) gives  $n \approx \sqrt{A_n/A_Q} \approx LA_Q^{-1/2}$ , hence a natural unit of length  $\ell_Q = A_Q^{1/2}$ . This fixes an absolute normalization for the signal correlation function,

$$\ell_Q = A_Q^{1/2} = \sqrt{2 \ln 2 \hbar G c^{-3} / \sqrt{3}} = 0.895 \ell_P \quad (37)$$

It could be that the appropriate fundamental unit to use in Eq. (35) is not  $\ell_P$ , but the loop-normalized Planck length  $\ell_Q$  (Eq. 37). They are almost the same, but in any case experiments should be designed with enough sensitivity to measure this value and attention to precise calibration. An experiment measures the absolute value of a fundamental length or time, and its exact value has information about its relation to  $G$ .

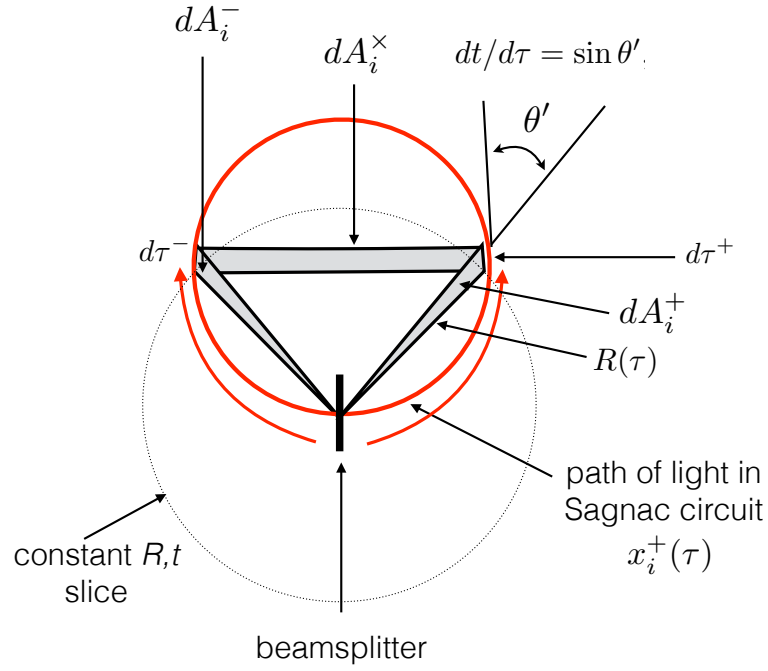


FIG. 3. Definitions of geometrical quantities used to project exotic correlations onto the affine time parameter  $\tau$  of the light path in a planar Sagnac circuit, in the rest frame of the beamsplitter (Eqs. 27, 28, 29, 33). For this illustration, the circuit is shown as a solid circle. The cross term  $A^\times$  is not included for pure rotational modes.

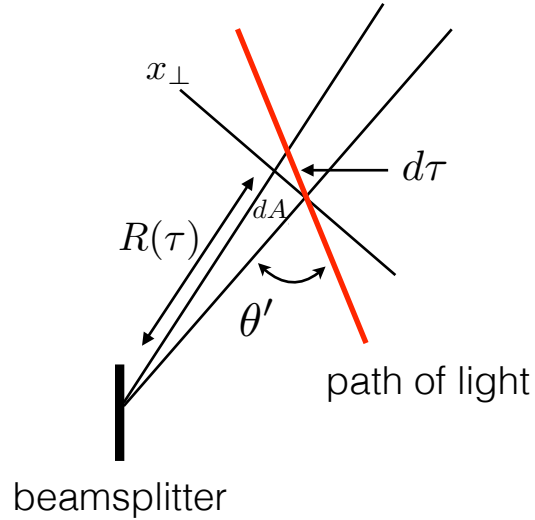


FIG. 4. Definitions of geometrical quantities for a straight portion of the light path in any planar interferometer in the rest frame of the beamsplitter.

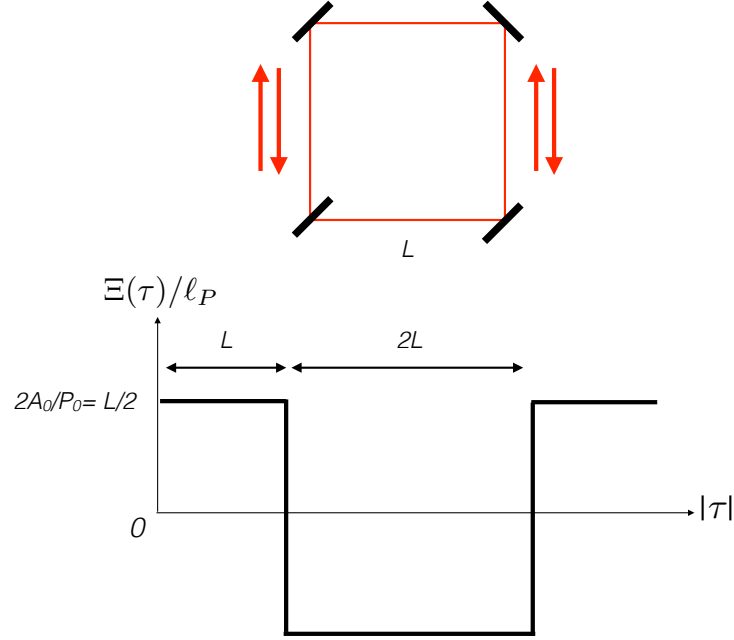


FIG. 5. Spatial layout and exotic signal correlation function for a square Sagnac interferometer. The general formula (Eq. 35) gives the signal correlation for a planar interferometer of any shape.

#### Classical Sagnac Effect

It is interesting to compare the exotic correlations with a similar derivation of the classical Sagnac effect. For an apparatus of any shape, the phase shift in length units between light going in two directions around a circuit rotating with angular velocity  $\omega_0$ , relative to the local nonrotating inertial frame, is

$$c\Delta t = 4A_0\omega_0/c. \quad (38)$$

This formula can be derived by summing the extra contributions from each straight photon path segment around a circuit. Let  $\delta t$  denote the “extra” propagation time for a photon—the extra time to the next reflection—in a small interval of a straight path, due to the fact that the apparatus is rotating. It is related to the transverse rotation  $d\delta x_\perp = R\omega_0 d\tau$  in the same interval by

$$cd\delta t/d\delta x_\perp = \sin\theta', \quad (39)$$

using the notation shown in Fig (4). Combining with the swept area (Eq. 30), the net time lag around a circuit is

$$c \int d\delta t = 2\omega_0 A_0/c. \quad (40)$$

The total Sagnac effect is twice this amount because it is the total difference between opposite directions.

The exotic effect produces the tiny fluctuations around this value, due to the imperfect definition of the frame. The exotic correlation amplitude for a Sagnac device on any scale (Eq. 36), which is a mean square displacement, is equal to the classical displacement for an apparatus rotating at angular velocity  $\omega_0 = c/2P_0$ , times the Planck length. Once again, the exotic phase displacement resembles approximately the value of displacement in a Planckian random walk, but with symmetries and projection factors appropriate to rotation.



## V. EXOTIC ROTATIONAL CORRELATIONS AND COSMIC ACCELERATION

The properties of the Planck scale rotational correlations are scale-free power laws, apart from the Planck scale itself. Systems in the real world have scales determined by the physics of matter fields. The previous discussion considers the effects of entanglement with geometrical states on field degrees of freedom, including the reconciliation with holographic gravity, and small phase displacements measurable in interferometers. The latter calculation is definite enough for a precise experimental test. We now consider estimates of a complementary effect: how entanglement of field vacuum and geometry could break the scale invariance of gravity, and account for the value of the scalar cosmological constant in the emergent classical field equations.

### The Cosmological Constant and Cosmic Acceleration

The Einstein field equations of general relativity can be contracted with the metric tensor  $g_{\mu\nu}$  to yield a scalar relation,

$$\Lambda = \frac{2\pi G}{c^4}(T + 2\mathcal{R}), \quad (41)$$

where  $\Lambda$  denotes the cosmological constant,  $\mathcal{R} \equiv R(c^4/16\pi G)$  denotes the Ricci curvature scalar  $R \equiv g^{\mu\nu} R_{\mu\nu}$  in units of  $16\pi G/c^4$ ,  $R_{\mu\nu}$  denotes the Ricci curvature tensor, and  $T$  denotes the trace of the classical energy momentum tensor of matter,  $T_{\mu\nu}$ . Within general relativity, there is no mathematical difference between  $\Lambda$  and a component of the matter field vacuum with  $T_{\mu\nu}$  proportional to  $g_{\mu\nu}$ . In standard theory,  $\Lambda$  is a new constant of nature, unconnected to other properties of gravity or matter[27]. Its value is also mysterious and arbitrary in holographic theories of gravity[42, 57].

Cosmic data suggest that the expansion of the universe is accelerating[58–61]. This phenomenon can be interpreted in classical General Relativity as an effect of  $\Lambda$ . In addition to the standard attractive gravity of normal forms of matter expressed in  $T$ , the cosmological term produces an additional repulsive acceleration between two bodies at separation  $r$ ,

$$\ddot{r} = H_\Lambda^2 r, \quad (42)$$

proportional to their separation  $r$  in Newtonian coordinates, where  $H_\Lambda^2 \equiv \Lambda/3$ . In cosmological models where matter has  $T > 0$ ,  $H_\Lambda$  is the asymptotic value of the Hubble expansion rate in the far future, after other forms of matter have thinned out due to the expansion. In other models, cosmic acceleration is caused by exotic new forms of “dark energy” with  $T < 0$ , whose gravity creates acceleration even with  $\Lambda = 0$ . Those models also introduce new fundamental scales of mass, generally unconnected with known physics [60–62].

### Cosmological Constant from Entanglement of Geometry with the Field Vacuum

#### *Cosmic Centrifugal Acceleration*

If matter and geometry are subsystems of a single quantum system, the standard distinction between matter ( $T$ ) and geometry ( $\mathcal{R}$ ) becomes ambiguous on scales where they are significantly entangled. As shown above, that happens in an energy dependent way for matter fields, at the Chandrasekhar radius for a given particle energy. It is natural to suggest that the value of  $\Lambda$  in the emergent classical description is set by entanglement of a special scale of the field vacuum with geometry.

We propose to interpret cosmic acceleration as an emergent kinematic property of space, associated with rotational fluctuations in the inertial frame and their entanglement with known matter fields. In this interpretation, the scale of cosmic acceleration is determined by known length scales already built into physics, the Planck scale and the strong interaction scale. On cosmological scales, the average effect is the same as a classical constant  $\Lambda$ . The most direct evidence for this mechanism would come from interferometric measurement of exotic rotational correlations on laboratory scales, as discussed above.

A simple starting point is to compare Eq. (42) with a classical system rotating at a rate  $\omega$ . A body at separation  $r$  from the axis of rotation experiences a centrifugal acceleration,

$$\ddot{r} = \omega^2 r. \quad (43)$$

Like cosmic acceleration (Eq. 42), it is independent of mass, always directed outwards, and proportional to  $r$ .

The two outward accelerations agree if  $\omega = H_\Lambda$ . However, it is well known that cosmic acceleration cannot simply be due to a classical centrifugal acceleration from rotation on a cosmic scale. Classical rotation is not isotropic, and the centrifugal effect from rotation at a rate  $\omega = H_\Lambda$  would cause large amplitude, large scale anisotropy of cosmic radiation and expansion that is not observed.

Cosmic acceleration could however be associated with rotational fluctuations on a much smaller scale. These average out in a large scale time or space average, so they do not conflict with cosmic isotropy data. Even if rotation has zero mean and fluctuates in random directions, its fluctuations always push outwards, so the mean square fluctuating component creates a net, secular centrifugal acceleration with a fluctuating directional component. Colloquially, we can say that the universe shakes apart.

Of course in Newtonian physics, an acceleration entails a force. Centrifugal acceleration can refer to a real force, as one experiences in a spinning merry-go-round, or a fictional one, as in a noninertial rotating frame. They refer to the same effect: because of the noninertial relationship between radial and tangential components of position in a rotating frame, a body that moves at a velocity that maintains a constant direction in a rotating frame accelerates outwards in the inertial frame. In an emergent geometry, the definition of an emergent acceleration is bound up with the definition of emergent position. Here, rather than interpreting cosmic acceleration as a new force, we interpret it as an emergent kinematical effect of exotic rotational correlations that describe Planckian deviations from inertial motion—the same mismatch between the local and cosmic inertial frames that leads to holographic noise in interferometers. The rotational fluctuations average to smaller values at large scales and long durations, but there may be a very small residual systematically outward-directed emergent radial acceleration.

#### *Absolute Value of $\Lambda$*

Clearly, the exotic fluctuations do not have an emergent centrifugal effect on all scales. If they did, everything would fly apart at the Planck rate. But there is a scale where the Planckian rotational acceleration matches the observed cosmic acceleration. As it turns out, that scale coincides with the Chandrasekhar scale for the structural scale of the strong interaction field vacuum. This coincidence suggests a heuristic explanation for the value of the cosmological constant.

As a rough estimate, start with the root-mean-square rate of Planckian rotational fluctuations at separation  $R$  given by Eq. (24) in Planck units,  $\omega_R = R^{-3/2}$ . Centrifugal acceleration thus matches cosmic acceleration—that is,  $\omega_R = H_\Lambda$ —for fluctuations of spatial extent

$$R_\Lambda \approx H_\Lambda^{-2/3}. \quad (44)$$

This is the Chandrasekhar-Planck entanglement radius (Eq. 8) for particle mass

$$m(R_C = R_\Lambda) = R_\Lambda^{-1/2} \approx H_\Lambda^{1/3}. \quad (45)$$

It has long been noticed that in Planck units,  $H_0^{1/3}$  approximately coincides with a proton or pion mass. A direct physical relationship between cosmological  $\Lambda$  and a strong interaction scale—for example,  $m_\pi \approx H_\Lambda^{1/3}$ —was posited long ago by Zeldovich[63], and more recently by Bjorken and others[64–68]. In the rotational-acceleration model, the connection is established, and the scale is set, via entanglement of the field vacuum with exotic geometrical rotational states. We conjecture that on small scales, rotational fluctuations are “virtual” in the sense that a net outward acceleration is not generated in the emergent space, but that above a scale  $R_\Lambda$  connected with strong interactions, entanglement with the field vacuum produces a universal secular radial acceleration. At a spatial scale of  $R_\Lambda$ , rotational fluctuations on a light crossing time, with transverse width about equal to the strong interaction scale, gives an rms angular rotation rate about equal to the Hubble constant.

The entanglement conjecture suggests a more precise way to relate the value of  $\Lambda$  to a field vacuum scale. The effective constant  $\Lambda$  in the classical field equation comes about from entanglement of the subsystems represented by matter  $T$  and curvature  $\mathcal{R}$ . In the classical view the total information in the system is expressed in holographic terms, the area of the event horizon as determined by  $\Lambda$ . The number of degrees of freedom of the cosmic system can be estimated in standard physics from the matter side or from the geometry side: the 3D information density for the field vacuum equals the mean 3D density of holographic information within the cosmic horizon[22, 57].

The number of gravitational degrees of freedom is one quarter of the area of the cosmic event horizon in Planck units, given by  $\pi H_\Lambda^{-2}$ . Dividing by the 3-volume gives the holographic information density

$$\mathcal{I}_\Lambda = 3H_\Lambda/4. \quad (46)$$

The density of field modes per 3D volume with a UV cutoff at  $k_{max}$  is

$$\mathcal{I}_f(k_{max}) = k_{max}^3 4\pi/3(2\pi)^3. \quad (47)$$

A scalar field therefore matches cosmic information (that is,  $\mathcal{I}_\Lambda = \mathcal{I}_f(k_{max})$ ) for a field cutoff at

$$k_{max} = k_\Lambda \equiv (H_\Lambda 9\pi^2/2)^{1/3}. \quad (48)$$

One estimate of  $H_\Lambda$  from current cosmological data[22, 61, 69] yields

$$H_\Lambda = \Omega_\Lambda^{1/2} H_0 = 0.99 \pm 0.018 \times 10^{-61} \quad (49)$$

in Planck units, where  $H_0$  denotes the current value of the Hubble constant and  $\Omega_\Lambda$  denotes the density parameter of the cosmological constant. (This value and error estimate are not meant to be definitive, but are taken to illustrate typical values of current measurements near the state of the art; the values chosen here correspond to  $h_0 = 0.738 \pm 0.024$  and  $\Omega_\Lambda = 0.7 \pm 0.01$  in standard cosmological notation.) The value of the field cutoff scale that matches this observed cosmological information density is

$$k_\Lambda = 1.65 \pm 0.01 \times 10^{-20} m_P = 201 \pm 1.2 \text{ MeV}. \quad (50)$$

This value is close to the characteristic scale  $\Lambda_{QCD}$  of the strong vacuum. Estimates of that scale, from theoretical extrapolation of measurements at higher energies[61], have a fractional systematic uncertainty comparable those of the cosmological measurements. Thus, within current systematic errors, the cosmic and matter information densities agree. The spatial coherence scale of the fluctuating rotational modes mainly responsible for the cosmic acceleration is about

$$R_\Lambda \approx k_\Lambda^{-2} = 3.7 \times 10^{39} = 60 \text{ km}. \quad (51)$$

In this scenario, the scale invariance of gravity is broken by the strong interactions. The effect of the field vacuum is imprinted here not by a new coupling or field potential, but by quantum entanglement of fields with geometry. The scale of cosmic acceleration is set by the imperfect emergence of the inertial frame—the scale where the directional information content of the field vacuum runs up against the Planck limit. In the cosmic system, exotic correlation maps the strong correlation length in 3D holographically onto the Planck length in 2D. Virtual rotation affects secular radial acceleration when localization in space of a field state over a Hubble time, the timescale for information from infinity to be refreshed, matches the natural scale for the cosmic expansion to “notice” the mismatch of local and cosmic inertial frames. At the radius  $R_\Lambda$ , incoming rotational cosmic information aligns the long term average with the cosmic inertial frame, leaving a residual centrifugal acceleration at larger radii. The information lost over the cosmic horizon matches the lost information in small scale rotational fluctuations.

It is clearly too simplistic to picture cosmic acceleration as simply due to the universe “shaking apart”, but there appears to be a plausible connection between two independently measurable phenomena that have no relationship in standard theory: the cosmological constant, and exotic correlations in interferometers. Since the rotational correlations could be confirmed in an experiment, the experimental program described here could provide a concrete clue to the link between Standard Model physics and cosmic acceleration.

Although the detailed underlying mechanism of entanglement has not been rigorously modeled, these heuristic arguments suggest that the absolute value of the cosmological constant is determined by already known elements of physics, without additional parameters, scales, or fields. The built-in cosmic acceleration timescale  $H_\Lambda^{-1}$  in this scenario depends on approximately the same combination of physical constants as a stellar lifetime, providing a natural resolution of the fine-tuning or “why now” problem [22, 70]. The values of the cosmological constant and strong interaction scale are not independent; thus, it is tempting to speculate that the well-understood logarithmic running of the strong coupling constant with energy scale is ultimately responsible for the exponentially large ratios of cosmic quantities to the Planck scale.

If this link is real, the absolute value of the cosmological constant becomes an important physical quantity to measure: it is no longer an arbitrary number, but has a value that can be compared precisely, using a yet-to-be-discovered fundamental theory, with locally measured properties of standard model interactions. In terms of conventional cosmological parameters, the important quantity is the product  $\Omega_\Lambda H_0^2$ . A similar remark applies to the absolute value of  $\Lambda_{QCD}$ ; its exact absolute value may be important to test fundamental theory, through precise comparison with  $\Lambda$ .

A new and unique feature of this scenario is that cosmic acceleration is not constant, but fluctuates. The systematic acceleration that we measure in cosmic data is a sum of fluctuating contributions from many small scale rotational fluctuations.

In principle, there must be a locally measurable, radial component to exotic Planck motion that was not included in the scale-free analysis used for the Sagnac interferometer. It corresponds to a monopole expansion mode of spatial motion, unlike the pure tensor modes associated with gravitational waves, or pure rotational modes associated with exotic Planck fluctuations, without the entanglement of the field vacuum. Unlike a standard cosmological constant, the radial component fluctuates. The fluctuations are not scale free, but have a characteristic temporal frequency at about  $c/R_\Lambda \approx 5000$  Hz, and a spatial coherence scale of about  $R_\Lambda \approx 60$  km. In principle, these distinctive features could enable a direct experimental test of this scenario for emergent cosmic acceleration. The temporal variation and spatial coherence distinguish it from classical backgrounds.

The effect could be measured using correlated signals between spatially separate, ground-based interferometers. Normally in gravitational wave observatories, the important signal is the dark port of the Michelson interferometer, which records the arm-length difference or strain mode associated with gravitational waves. For cosmic gravitational wave sources, this signal is correlated over large interferometer separations. Here, we are interested in another signal, the common-mode or bright port signal associated with a breathing mode, which measures the sum of the arms. It should have significant power only at low frequencies (below about 5000 Hz), and should be correlated spatially only for interferometers within about 60 km of each other. This unusual combination of correlation features— a signature of emergent, quantum cosmic acceleration— is unlike any well known classical source of signal correlation.

The heuristic picture above allows a quantitative estimate of the magnitude of the effect. For an apparatus of size  $R_\Lambda$ , the radial velocity increases in time  $R_\Lambda/c$  by an amount  $\Delta v \approx H_\Lambda^2 R_\Lambda^2/c$ , which is also the typical fluctuation. This leads to a positional displacement difference by about  $\Delta x \approx H_\Lambda^2 R_\Lambda^3/c^2$ , which according to Eq. (44) is only about one Planck length. The sensitivity required to detect this effect is of course far beyond that of gravitational wave observatories[71].

This result also suggests that the exotic Sagnac correlation derived above (Eq. 35) is little affected by matter entanglement, and should apply also for interferometers much larger than  $R_\Lambda$ . It could also be that measurable modifications occur, for example, the cross term (Eq. 29) may no longer vanish. It could be tested in this regime by a long baseline interferometer in space, similar to proposed designs for the Laser Interferometer Space Antenna. In a triangle configuration of satellites, combinations of signals can be combined to yield estimates of all modes of motion— strain, shear, expansion, and rotation, including Sagnac modes[20, 72]. A more advanced design (e.g. ref. [73]) may be needed to isolate the exotic noise from actual sources of gravitational waves.

In this context it is useful to provide estimates of the exotic fluctuations in the units of broad band noise intensity most familiar in these studies, the broad band density in a stochastic background of gravitational waves,  $\Omega_{GW} = \rho_{GW}/\rho_{crit}$ . In Planck units, the cosmic critical density is  $\rho_{crit} \approx H_\Lambda^2$ . The exotic correlations create an equivalent metric strain  $h \approx R^{-1/2}$  at separation  $R$ , so their equivalent apparent density at frequency  $f = R^{-1}$  is  $\rho_{\Xi GW} \approx h^2 f^2 \approx R^{-3}$ , that is, one Planck mass per volume  $R^3$ . In cosmic units, using  $R_\Lambda \approx H_\Lambda^{-2/3}$  we have  $\Omega_{\Xi GW} = \rho_{\Xi GW}/\rho_{crit} \approx (R/R_\Lambda)^{-3}$ . Thus on the scale  $R_\Lambda$  the apparent density of holographic noise in a Sagnac interferometer is about the same as a critical density of gravitational waves, while at higher frequencies (that is, above about 5000 Hz), it mimics a much higher density.

The heuristic model suggests an even more exotic correlation, in cosmic acceleration of distant sources. That is, there should be a small fluctuating part of cosmic acceleration in common to all cosmic sources. The contribution from the local rotational fluctuation is highly correlated for sources at all redshifts across large angles of the sky, with a pattern that is almost the same for measurements at the same time at observatories within 60 km of each other. This unusual form of quantum correlation is also a unique and distinctive signature of the proposed scenario, but again is not practical to implement in a real experiment. The acceleration of cosmic sources with time fluctuates at  $\approx 5000$  Hz; the fluctuation amplitude in distance on this timescale is only about one Planck length.

## ACKNOWLEDGMENTS

This work was supported by the Department of Energy at Fermilab under Contract No. DE-AC02-07CH11359. The author is grateful for the hospitality of the Aspen Center for Physics, which is supported by National Science

- 
- [1] C. Rovelli, *Quantum Gravity* (Cambridge University Press, 2004).
- [2] T. Thiemann, *Modern Canonical Quantum General Relativity* (Cambridge University Press, 2008) arXiv:gr-qc/0110034 [gr-qc].
- [3] A. Ashtekar, PoS **QGQGS2011**, 001 (2011), arXiv:1201.4598 [gr-qc].
- [4] T. Mohaupt, in *Quantum Gravity: From Theory to Experimental Search*, Lecture Notes in Physics, Vol. 631, edited by D. Giulini, C. Kiefer, and C. Lämmerzahl (Springer, Berlin; New York, 2003) pp. 173–251, arXiv:hep-th/0207249.
- [5] S. Weinberg, *The Quantum Theory of Fields* (Cambridge University Press, 1996).
- [6] F. Wilczek, Rev. Mod. Phys. **71**, S85 (1999).
- [7] J. Polchinski, *String Theory* (Cambridge University Press, 1998).
- [8] J. H. Schwarz, “Introduction to superstring theory,” (2000), arXiv:hep-ex/0008017.
- [9] M. R. Douglas and N. A. Nekrasov, Rev. Mod. Phys. **73**, 977 (2001).
- [10] S. Hossenfelder, Living Rev. Rel. **16**, 2 (2013).
- [11] Y. J. Ng and H. van Dam, Found. Phys. **30**, 795 (2000), arXiv:gr-qc/9906003 [gr-qc].
- [12] G. Amelino-Camelia, Phys. Rev. D **62**, 024015 (2000).
- [13] G. Amelino-Camelia, (2001), arXiv:gr-qc/0104005 [gr-qc].
- [14] G. Amelino-Camelia, Living Reviews in Relativity **16** (2013), 10.12942/lrr-2013-5.
- [15] O. Kwon and C. J. Hogan, “Interferometric Probes of Planckian Quantum Geometry,” ArXiv:1410.8197 [gr-qc].
- [16] C. J. Hogan, Phys. Rev. **D77**, 104031 (2008).
- [17] C. J. Hogan, Phys. Rev. **D78**, 087501 (2008).
- [18] C. J. Hogan, Phys. Rev. **D85**, 064007 (2012).
- [19] C. J. Hogan, “Directional entanglement of quantum fields with quantum geometry,” ArXiv:1312.7798 [gr-qc].
- [20] C. Hogan, in *9th LISA Symposium*, Astronomical Society of the Pacific Conference Series, Vol. 467, edited by G. Auger, P. Binétruy, and E. Plagnol (2013) p. 17, arXiv:1208.3703 [quant-ph].
- [21] C. J. Hogan and O. Kwon, (2015), arXiv:1506.06808 [gr-qc].
- [22] C. J. Hogan, “Quantum Entanglement of Matter and Geometry in Large Systems,” (2014), arXiv:1412.1807 [gr-qc].
- [23] H. Salecker and E. P. Wigner, Physical Review **109**, 571 (1958).
- [24] E. J. Post, Rev. Mod. Phys. **39**, 475 (1967).
- [25] K. U. Schreiber, A. Gebauer, H. Igel, J. Wassermann, R. B. Hurst, and J.-P. R. Wells, Comptes Rendus Physique **15**, 859 (2014), the Sagnac effect: 100 years later / L’effet Sagnac : 100 ans après.
- [26] A. S. Chou *et al.*, (2015), arXiv:1512.01216 [gr-qc].
- [27] S. Weinberg, Rev. Mod. Phys. **61**, 1 (1989).
- [28] A. Zeilinger, Rev. Mod. Phys. **71**, S288 (1999).
- [29] Č. Brukner and A. Zeilinger, Foundations of Physics **39**, 677 (2009), arXiv:0905.0653 [quant-ph].
- [30] S. Chandrasekhar, Astrophys. J. **74**, 81 (1931).
- [31] A. G. Cohen, D. B. Kaplan, and A. E. Nelson, Phys. Rev. Lett. **82**, 4971 (1999).
- [32] J. M. Bardeen, B. Carter, and S. Hawking, Commun. Math. Phys. **31**, 161 (1973).
- [33] J. D. Bekenstein, Phys. Rev. **D7**, 2333 (1973).
- [34] J. D. Bekenstein, Phys. Rev. **D9**, 3292 (1974).
- [35] S. Hawking, Nature **248**, 30 (1974).
- [36] S. Hawking, Commun. Math. Phys. **43**, 199 (1975).
- [37] G. ’t Hooft, “Dimensional Reduction in Quantum Gravity,” ArXiv:gr-qc/9310026.
- [38] L. Susskind, J. Math. Phys. **36**, 6377 (1995).
- [39] R. Bousso, Rev. Mod. Phys. **74**, 825 (2002), arXiv:hep-th/0203101 [hep-th].
- [40] J. M. Maldacena, Adv. Theor. Math. Phys. **2**, 231 (1998).
- [41] Horowitz, G. T. and Polchinski, J., (2006), gr-qc/0602037.
- [42] T. Jacobson, Phys. Rev. Lett. **75**, 1260 (1995).
- [43] E. Verlinde, JHEP **1104**, 029 (2011).
- [44] T. Padmanabhan, Gen. Rel. Grav. **46**, 1673 (2014), arXiv:1312.3253 [gr-qc].
- [45] N. Margolus and L. B. Levitin, *4th Workshop on Physics and Computation (PhysComp 96) Boston, Massachusetts, November 22-24, 1996*, Physica **D120**, 188 (1998), arXiv:quant-ph/9710043 [quant-ph].
- [46] S. Lloyd, (2012), arXiv:1206.6559 [gr-qc].
- [47] C. M. Caves, Phys. Rev. Lett. **45**, 75 (1980).
- [48] C. M. Caves, Phys. Rev. **D23**, 1693 (1980).
- [49] C. M. Caves, K. S. Thorne, R. W. P. Drever, V. D. Sandberg, and M. Zimmermann, Rev. Mod. Phys. **52**, 341 (1980).
- [50] C. Gardiner and P. Zoller, *Quantum Noise: A Handbook of Markovian and Non-Markovian Quantum Stochastic Methods with Applications to Quantum Optics*, Springer Series in Synergetics (2004).
- [51] A. Ashtekar, J. C. Baez, and K. Krasnov, Adv. Theor. Math. Phys. **4**, 1 (2000), arXiv:gr-qc/0005126 [gr-qc].
- [52] A. Ashtekar, J. Baez, A. Corichi, and K. Krasnov, Phys. Rev. Lett. **80**, 904 (1998), arXiv:gr-qc/9710007 [gr-qc].

- [53] I. Newton, trans. A. Motte (1729) and F. Cajori (1934), *Philosophiae Naturalis Principia Mathematica* (University of California Press, 1934).
- [54] R. Rynasiewicz, in *The Stanford Encyclopedia of Philosophy*, edited by E. N. Zalta (2014) summer 2014 ed.
- [55] R. DiSalle, in *The Stanford Encyclopedia of Philosophy*, edited by E. N. Zalta (2009) winter 2009 ed.
- [56] T. Padmanabhan, *Class. Quan. Grav.* **4**, L107 (1987).
- [57] T. Padmanabhan and H. Padmanabhan, *International Journal of Modern Physics D* **23**, 1430011 (2014), arXiv:1404.2284 [gr-qc].
- [58] A. G. Riess *et al.* (Supernova Search Team), *Astron. J.* **116**, 1009 (1998), arXiv:astro-ph/9805201 [astro-ph].
- [59] S. Perlmutter *et al.* (Supernova Cosmology Project), *Astrophys. J.* **517**, 565 (1999), arXiv:astro-ph/9812133 [astro-ph].
- [60] J. Frieman, M. Turner, and D. Huterer, *Ann. Rev. Astron. Astrophys.* **46**, 385 (2008), arXiv:0803.0982 [astro-ph].
- [61] K. A. Olive, *et al.* (Particle Data Group), *Chin. Phys.* **C38**, 090001 (2014).
- [62] A. Joyce, B. Jain, J. Khoury, and M. Trodden, *Phys. Rept.* **568**, 1 (2015), arXiv:1407.0059 [astro-ph.CO].
- [63] Y. B. Zeldovich, *Physics-Uspekhi* **11**, 381 (1968).
- [64] J. D. Bjorken, in *Proceedings, 5th Meeting on CPT and Lorentz Symmetry (CPT 10)* (2010) pp. 1–5, arXiv:1008.0033 [hep-ph].
- [65] J. D. Bjorken, *Phys. Rev.* **D67**, 043508 (2003), arXiv:hep-th/0210202 [hep-th].
- [66] A. Randono, *Gen. Rel. Grav.* **42**, 1909 (2010), arXiv:0805.2955 [gr-qc].
- [67] S. Carneiro, *Int. J. Mod. Phys.* **D12**, 1669 (2003), arXiv:gr-qc/0305081 [gr-qc].
- [68] R. Schutzhold, *Phys. Rev. Lett.* **89**, 081302 (2002), arXiv:gr-qc/0204018 [gr-qc].
- [69] A. G. Riess, L. Macri, S. Casertano, H. Lampeitl, H. C. Ferguson, A. V. Filippenko, S. W. Jha, W. Li, and R. Chornock, *Astrophys. J.* **730**, 119 (2011), [Erratum: *Astrophys. J.* 732,129(2011)], arXiv:1103.2976 [astro-ph.CO].
- [70] C. J. Hogan, *Rev. Mod. Phys.* **72**, 1149 (2000), arXiv:astro-ph/9909295 [astro-ph].
- [71] R. X. Adhikari, *Reviews of Modern Physics* **86**, 121 (2014), arXiv:1305.5188 [gr-qc].
- [72] C. J. Hogan and P. L. Bender, *Phys. Rev.* **D64**, 062002 (2001), arXiv:astro-ph/0104266 [astro-ph].
- [73] C. Cutler and D. E. Holz, *Phys. Rev. D* **80**, 104009 (2009), arXiv:0906.3752 [astro-ph.CO].
- [74] A. Connes, *Noncommutative Geometry* (Academic Press, 1994).
- [75] A. Connes and M. Marcolli, “A Walk in the Noncommutative Garden,” ArXiv:math/0601054.
- [76] N. Seiberg and E. Witten, *JHEP* **9909**, 032 (1999).
- [77] L. D. Landau and E. M. Lifshitz, *Quantum Mechanics: Non-Relativistic Theory*, 3rd ed. (Pergamon, Oxford, 1977) sections 26 & 27.
- [78] G. E. Stedman, *Reports on Progress in Physics* **60**, 615 (1997).
- [79] B. Culshaw, *Measurement Science and Technology* **17**, R1 (2006).
- [80] A. A. Michelson and H. G. Gale, *Astrophys. J.* **61**, 140 (1925).

## Appendix A: A Toy Model of Quantum Geometrical States: Spin Algebra of Quantum Position Operators

This appendix summarizes a simple, antisymmetric spin algebra commutator of 3-dimensional position operators that serves as a toy model for a quantum-geometrical correlation of positions (Eq. 26). It relates a holographic density of position states to a fundamental length, and derives the transverse variance of the position wave function used above to estimate the Sagnac correlation function (Eqs. 32, 35) and rotational fluctuations (Eq. 24). Apart from the Planckian coefficients in place of  $\hbar$ , most of the algebra here is found in the literature on quantum angular momentum. It is quoted here for convenience, updating a similar summary in ref. [21].

This system is a model of geometrical states. It includes no model of dynamics, and also has no direct relation to the standard literature on noncommutative geometry or fields[9, 74–76]. However, it provides a consistent holographic quantum model for macroscopic geometrical relationships of Planck scale elements in three dimensions. The main point is to display explicitly a quantum system where the three dimensions of space map onto two dimensions, one radial/longitudinal and one directional. The mapping is the same as that for spins: the radial position dimension corresponds to the total angular momentum, and the directional position dimension corresponds to its projection onto any axis.

Consider position operators  $\hat{x}_i$  that obey the standard spin algebra with Planck scale commutator:

$$[\hat{x}_i, \hat{x}_j] = \hat{x}_k \epsilon_{ijk} i \ell_P. \quad (\text{A1})$$

These represent quantum-geometrical objects in three spatial dimensions. Their wave functions live on a single spacelike hypersurface. They represent projections of world line wave functions; that is, the 3-D correlation is

$$\Xi_{ij}(x_k, \tau = 0) = \epsilon_{ijk} x_k \ell_P, \quad (\text{A2})$$

which is the basis of the correlation analysis above (Eq. 26). This system can be analyzed in exactly the same way as standard angular momenta, albeit with a completely different physical application.

In analogy with the total angular momentum in a spin system, define a “separation operator”, that has dimensions of area:

$$|\hat{x}|^2 \equiv \hat{x}_i \hat{x}_i, \quad (\text{A3})$$

It commutes with  $\hat{x}_i$  operators, so it behaves classically:

$$[|\hat{x}|^2, \hat{x}_i] = 0, \quad (\text{A4})$$

This operator takes discrete eigenvalues:

$$|\hat{x}|^2 |l\rangle = l(l+1)\ell_P^2 |l\rangle. \quad (\text{A5})$$

The discrete eigenvalues correspond to classical values of separation  $R$  according to:

$$R^2 \equiv l(l+1)\ell_P^2 \approx l^2 \ell_P^2 \quad (\text{A6})$$

where  $l$  are positive integers, quantum numbers of eigenstates of  $|\hat{x}|^2$ .

Let  $l_i$  denote eigenvalues of position components projected in direction  $i$ . In a state  $|l\rangle$  of separation number  $l$ , the projected position operator  $\hat{x}_i$  can have eigenvalues in units of  $\ell_P$ ,

$$l_i = l, l-1, \dots, -l, \quad (\text{A7})$$

giving  $2l+1$  possible values. In an eigenstate with a definite value of position in direction  $i$ ,

$$\hat{x}_i |l, l_i\rangle = l_i \ell_P |l, l_i\rangle. \quad (\text{A8})$$

The total number of position eigenstates in a 3-sphere is

$$\mathcal{N}_{Q3S}(R) = \sum_{l=1}^{l_R} (2l+1) = l_R(l_R+2) = (R/\ell_P)^2, \quad (\text{A9})$$

where the last equality applies in the large  $l$  limit. Thus, the number of quantum-geometrical position eigenstates in a volume scales holographically, as the surface area in Planck units. This simple model of quantization closely resembles (but is not exactly the same as) the spectrum of area states more rigorously derived within the framework of loop quantum gravity (Eq. 17).

Direct calculation (e.g., ref.[77]) also leads to the following product of amplitudes for measurements of either of the transverse components  $\hat{x}_j$ , with  $j \neq i$ :

$$\langle l_i | \hat{x}_j | l_i - 1 \rangle \langle l_i - 1 | \hat{x}_j | l_i \rangle = (l + l_i)(l - l_i + 1) \ell_P^2 / 2, \quad (\text{A10})$$

again for any  $i$ . The left side of equation (A10) can be interpreted as the expected value for the operator

$$\hat{x}_j |l_i - 1\rangle \langle l_i - 1| \hat{x}_j, \quad (\text{A11})$$

that is, a projection of position components  $j \neq i$  in a state  $|l_i\rangle$  of definite  $\hat{x}_i$ .

For  $l \gg 1$  and  $l_i \approx l$ — that is, a separation much larger than the Planck length— this corresponds to the expected variance in components of position transverse to separation:

$$\langle \hat{x}_j | l_i - 1 \rangle \langle l_i - 1 | \hat{x}_j \rangle \rightarrow \langle \hat{x}_j^2 \rangle. \quad (\text{A12})$$

Let  $\hat{x}_\perp$  denote a projection operator onto in any direction transverse to separation. We can rewrite this as a formula for the variance of the wave function, given by the right hand side of Eq. (A10) in the limit of  $l \gg 1$ , for  $l \pm l_i = 1$  (or indeed for any value of  $|l - l_i| \ll l^{1/2}$ ):

$$\langle \hat{x}_\perp^2 \rangle = R \ell_P. \quad (\text{A13})$$

This simple result is used above to set the scale of transverse position variance in phenomenological estimates, for example in Eqs. (32) and (24). The corresponding variance in direction is just  $\langle \hat{x}_\perp^2 \rangle / R^2 = \ell_P / R$ .

The same algebra can be applied to actual angular momentum. With  $j$  and  $\hbar$  in place of  $x$  and  $\ell_P$ , the width of the wave function for measured transverse components of standard angular momentum, in the limit of large  $|j|$ , is given by:

$$\langle \hat{j}_\perp^2 \rangle = |j| \hbar. \quad (\text{A14})$$

This simple formula describes a standard uncertainty in the direction in the limit of large angular momentum.

*Covariant Formulation in 4D*

The use of causal diamonds to define the entanglement between matter and geometry allows a covariant formulation in 4D that reduces to Eq. (A1) in the rest frame of a world line. Again, quantum operators are defined relative to a specific world line that defines a frame and a spatial origin. Lorentz invariance is broken by choice of world line, which projects the state onto a definite frame, but the state itself, and the physics, are fully diffeomorphism invariant.

The covariant quantum commutator relating position operators can be written as[20]:

$$[\hat{x}_\mu, \hat{x}_\nu] = \hat{x}^\kappa \hat{U}^\lambda \epsilon_{\mu\nu\kappa\lambda} i \ell_P, \quad (\text{A15})$$

where indices  $\mu, \nu, \kappa, \lambda$  run from 0 to 3 with the usual summation convention,  $\hat{U}$  represents an operator with the same transformation properties (in the classical limit) as the dimensionless 4-velocity of the body, and  $\epsilon_{\mu\nu\lambda\kappa}$  is the antisymmetric 4-tensor.

Eq. (A15) has a manifestly covariant classical interpretation, where the operators map onto their classical counterparts. In the low velocity limit, it becomes Eq. (A1). Their physical interpretation, as position operators relative to a specific world line, distinguishes this idea from standard noncommutative geometry.

The covariant formulation expresses how the commutation relations appear in a moving frame; the position operators transform consistently into standard 4D classical coordinates in the continuum limit. The theory is still not complete, since it has not been proven that quantum operators  $\hat{U}^\lambda$  define a consistent quantum algebra. We can write an expression  $\hat{U}^\lambda \equiv \hat{x}^\lambda (\hat{x}_\alpha \hat{x}^\alpha)^{-1/2}$  with the same form, in the classical limit, as the dimensionless 4-velocity of the body, normalized to preserve reparametrization invariance, where  $\dot{x} \equiv \partial x / \partial \tau$  and  $\tau$  denotes proper time. However, a fundamental operator equation should use only the  $\hat{x}_0$  coordinate, not a classical proper time. Thus, the time projections of the phenomenological derivations above are not rigorously derived here from a fully quantum theory.

### Appendix B: Experiment Concept: Superluminally Cross-Correlated, Colocated Sagnac Interferometers

The exotic rotational correlation (Eq. 35) may be detectable using an apparatus similar to the Fermilab Holometer[26], reconfigured to measure pure rotational modes. The Holometer achieves the sensitivity needed to measure exotic quantum-geometrical correlations by sampling and cross-correlating signals, from two separate but spatially adjacent power-recycled Michelson interferometers, at superluminal rates— that is, many times per light-crossing. A measurement of the exotic rotational correlation could be achieved with a similar experiment, configured as two interferometers that enclose overlapping areas. To achieve shot-noise-limited sensitivity, such a device would require superluminally correlated power-recycled interferometer cavities that include transverse segments far from the beamsplitter— for example, by bending the existing Michelson arms, or by enclosing a complete circuit, as in a Sagnac configuration.

The most advanced Sagnac interferometers operating today are active ring laser systems optimized for much lower frequencies, and used in ultra high precision applications such as geodesy [24, 78]. Sagnac interferometers are sometimes made with circuits of optical fibers[79]. Although in some ways that option is much simpler than the power-recycled cavity, it is not considered here, partly because shot noise limited performance at high power has not been demonstrated as it has for cavities. Sagnac-configured gravitational wave detectors are also possible, as in some designs for the Laser Interferometer Space Antenna[72].

It is useful to consider some concrete numbers for a system that could actually be built with modest resources. The size of the experimental apparatus is determined by a trade between competing effects: a larger device probes lower frequencies, where photon shot noise is smaller compared to the signal, but technical and environmental noises are larger. The parameters of the system chosen for illustration here are based on the successful demonstration[26] of shot-noise-limited performance in the Holometer at the same frequency, which yields sufficient sensitivity to measure the predicted correlation.

In the following, unless explicitly stated, units of length and time are Planck values  $\ell_P = \sqrt{\hbar G / c^3} = 1.616 \times 10^{-35}$  meters,  $t_P = \sqrt{\hbar G / c^5} = 5.4 \times 10^{-44}$  seconds.

- Two square Sagnac interferometers, each 20 meters on a side,  $L = 1.2 \times 10^{36}$ , are placed so their areas substantially overlap. Signals are cross correlated to separate the in-common exotic correlations from standard forms of uncorrelated quantum and technical noise.
- Each is a resonant power-recycled cavity to reduce shot noise.
- The area is 400 square meters,  $A_0 = L^2 = 1.5 \times 10^{72}$ .



- The perimeter is 80 meters,  $P_0 = 5 \times 10^{36}$ .
- With normalization the standard Planck length, the rms fluctuation in phase at the beamsplitter (Eq. 36) is  $\Xi_0^{1/2} = (2A_0/P_0)^{1/2} = 8 \times 10^{17} = 1.2 \times 10^{-17}$  meters, or 12 attometers, a level measurable with Holometer technology. With the Loop Quantum Gravity normalization (Eq. 37), it is smaller by a factor of  $\sqrt{\ell_Q/\ell_P} = 0.946$ . The absolute value of the correlation carries information about details of new Planck scale physics, which motivates absolute calibration at better than a few percent precision.
- The spacing (Eq. 21) between loop area states for the 400 square meter total area eigenstate is  $\Delta A = 2L\ell_Q = 2 \times 10^{36} = 5 \times 10^{-34} \text{m}^2 = 23$  square attometers.
- The equivalent angular rotation rate corresponding to the correlation amplitude is about

$$\langle \omega^2 \rangle^{1/2} = 2\pi(2A_0/P_0)^{1/2}P_0^{-2} = 2 \times 10^{-55} = 3.7 \times 10^{-12} \text{ Hz}, \quad (\text{B1})$$

or about one radian per  $10^4$  years.

- The peak frequency of the signal fluctuation spectrum (the Fourier transform of Eq. 35) occurs at about  $f \approx P_0^{-1} = 2 \times 10^{-37} = 4$  MHz. As in the Holometer, a high bandwidth sampling and correlation system is necessary to measure broad band spectra well below photon shot noise.
- The classical phase shift between the two directions around the circuit, from the earth's rotation, first measured in ref. [80], is

$$\delta\phi/2\pi = c\Delta t/\lambda = 4A_0\omega_{earth} \sin(\theta_{lat})/c = 3.9 \times 10^{-4}, \quad (\text{B2})$$

using Eq. (38), laser wavelength  $\lambda = 10^{-6}$  m, and the latitude of Fermilab,  $\theta_{lat} = 42$  degrees.